Int. J. Electrochem. Sci., 9 **(2014)** 6266 - 6280

International Journal of
ELECTROCHEMICAL
SCIENCE
www.electrochemsci.org

The Influence of Cathodic Polarization on Performance of Two Epoxy Coatings on Steel

Li Zhang, Xiangyu Lu, Yu Zuo[*]

Beijing Key Laboratory of Electrochemical Process and Technology for Materials, Beijing University of Chemical Technology, Beijing 100029, China
[*]E-mail: zuoy@mail.buct.edu.cn

Received: 23 June 2014 / *Accepted:* 28 July 2014 / *Published:* 25 August 2014

The influences of cathodic polarization on the failure process of two coatings, an epoxy coating and a 80wt% zinc-rich epoxy coating, on mild steel were studied with the methods of electrochemical impedance spectroscopy (EIS), scanning electron microscope (SEM) and Fourier transform infrared spectroscopy (FT-IR), in order to understand the effect of cathodic protection on coating performance. The application of cathodic polarization at −0.9 V_{SCE} on the epoxy coating increases the extent of degradation and reduces the protective properties of the coating, which may be attributed to the strengthened basic environment at the coating/metal interface due to cathodic polarization. While for the zinc-rich epoxy coating, cathodic polarization at −0.9 V_{SCE} decreases the dissolution rate of the zinc particles in coating and increases the coating resistance. The activation of zinc particles is delayed and the cathodic protection time contributed by the zinc particles is prolonged. As the result the performance of zinc-rich epoxy coating is improved by cathodic polarization.

Keywords: Cathodic polarization; Epoxy coating; Zinc-rich coating; EIS; Performance

1. INTRODUCTION

In marine environments cathodic protection (CP) is frequently combined with organic coatings to protect metallic structures [1,2]. With such application, the protection current density during CP is greatly decreased [3], and the performance of the coating system is also extended. However, the application of CP would generate hydroxyl ions on the cathodic surface, leading to strong alkalinity at the coating/substrate interface. Alkalization is the predominant reason for cathodic disbonding which can also be accelerated by the peroxides and free radicals formed by the cathodic reaction [4]. Some studies have focused on the influence of CP on organic coatings. Compared with the samples without CP, those coating systems under CP show smaller water diffusion coefficients and a further water

uptake process after the saturation [2]. Thu [5] found that a solvent-free coating exhibited the best compatibility with cathodic protection. Elta [6] reported that the application of cathodic protection at −1.1 V affected the protective properties of the coating, causing the coating resistance to fall, and the water uptake of the coated specimens was increased as a result of the increasing level of CP. Elta et al. [7] also studied the effects of CP on the mobility of Na^+, Ca^{2+}, and K^+ cations through the coating. The migration of these cations was shown to increase in the order $Ca^{2+} < Na^+ < K^+$ and the deterioration of the coating was found to increase in the same order.

Zinc- rich paints (ZRPs) are widely used primers with active pigments in which zinc particles are electrochemically more active than steel substrate and provide cathodic protection for the substrate [8]. On the other hand, applied cathodic protection is widely used in marine engineering. In some cases both ZRPs and applied cathodic protection are applied in order to obtain better protection for steel structures and ships [9,10]. However, there were few studies reporting the influence of cathodic protection on primers with active pigments which can provide cathodic protection for the substrate by themselves. In this paper, the effect of cathodic protection on the failure of a zinc-rich paint is investigated.

2. EXPERIMENTAL

2.1. Materials and samples preparation

Q235 carbon steel was cut into the size of 150×70×2 mm. The samples were ground using SiC abrasive paper up to 120 grit. The steel substrate was washed in distilled water and acetone in turn, then dried in air. The details of the formulation, experimental condition and thickness of four different samples examined in this study are listed in Table 1. The coatings were applied on the panels by manual brushing. Samples C and D were coated with a zinc-rich epoxy paint (881-X) that was obtained from Beijing BIAM New Materials Co and zinc represents 80 wt% on dry film. Samples named A and B were coated with epoxy coating which was a two component commercial epoxy-polyurethane (KFH-01) from Goldfish paint factory, Shijiazhuang, China.

2.2. Experimental condition

Two different continuous immersion conditions were chosen: open circuit potential (OCP) for samples A and C, and cathodic polarization (CP) at the potential of −0.9 V_{SCE} by a potentiostat for samples B and D. The potential of −0.9 V_{SCE} was selected because this potential is frequently applied for cathodic protection of carbon steels. The samples were immersed in 3.5 wt% NaCl solution (pH = 7) which was open to the air and renewed every two weeks. The reference electrode was a saturated calomel electrode and the counter electrode was graphite. For the EIS and open circuit potential (E_{OCP}) experiments, the measurements were carried out 15 min after the samples were removed from the cathodic polarization state.

Table 1. Thickness of the coatings and the testing conditions

Sample	Coating	Thickness / μm	Experimental condition
A	Epoxy coating	60 ± 5	Without CP
B	Epoxy coating	60 ± 5	CP
C	ZRP	120 ± 5	Without CP
D	ZRP	120 ± 5	CP

2.3. Measurements

Electrochemical impedance measurements were carried out in 3.5 wt% NaCl solution with a PARSTAT 2273 system, over the frequency range from 100 kHz to 0.01 Hz at open circuit potential with a 10 mV potential perturbation. The exposed working area was about 10 cm^2. A three-electrode arrangement was used, consisting of a saturated calomel electrode (SCE) as reference electrode, a platinum electrode as counter electrode, and a coated sample as the working electrode. Fitting of the impedance spectra was made using ZSimpWin software. To obtain more precise fitting results, the capacitive responses were fitted by constant phase elements, Q, whose impedance is defined as $Z_Q = \frac{1}{Y_D(j2\pi f)^n}$, in which Y_D is the CPE constant, j =√-1, f is the frequency (Hz) and the exponent n =α/(π/2), α being the phase angle of the CPE (radians). The E_{OCP} of sample D was measured in following way: a cathodic potential of -0.9 V_{SCE} was applied to the sample. At different time, the applied potential was removed and the open circuit potential was measured after 30 min. Then the cathodic polarization was applied again.

The epoxy coating sample and the ZRP sample were immersed in 3.5 wt% NaCl solution for 30 days and 47 days respectively. After immersion the coatings were peeled off from the substrate and a Hitachi S4700 field emission scanning electron microscope was used to characterize the back morphology of the coatings. The operating potential of the field emission source was 20 kV. The samples were coated with gold to preclude the charging effect during measurement. A Fourier transform infrared spectrophotometer (FT-IR, TENSOR-27, Germany) was used to analyze the structure variation of the coatings. The spectral resolution was 4 cm^{-1}, and the number of the scans was 30. X-ray photoelectron spectroscopy (XPS) was used to analyze the substrate surface after the epoxy coating was removed from the steel substrate. XPS measurements were performed using an ESCALAB250 instrument with a monochromatized Al Kα line (1486 eV) as the excitation source. All the binding energy values were calibrated according to C 1s peak at 285 eV. The narrow scan spectra were fitted with XPSPEAK 4.1 software.

3. RESULTS AND DISCUSSION

3.1. SEM observation

Fig. 1 shows the back morphology of the epoxy coating after immersion with or without CP. For the epoxy coating with CP holes are seen (Fig. 1a) while no visible holes can be found in the

epoxy coating without CP (Fig. 1b). Cathodic polarization may lead the cathodic surface to become alkaline by oxygen reduction: $2H_2O+O_2+4e \rightarrow 4OH^-$.

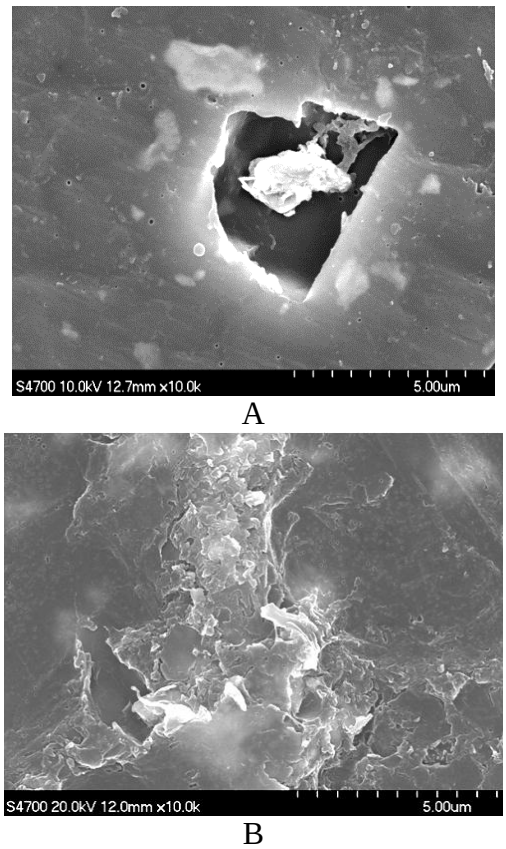

Figure 1. Back morphology of the epoxy coating after 30 days of immersion in 3.5% NaCl solution, (a) Under cathodic polarization, (b) At open circuit potential

Previous research has proved that the strong alkalinity and radicals could cause hydrolysis of the coating itself, resulting in depolymerization [11].

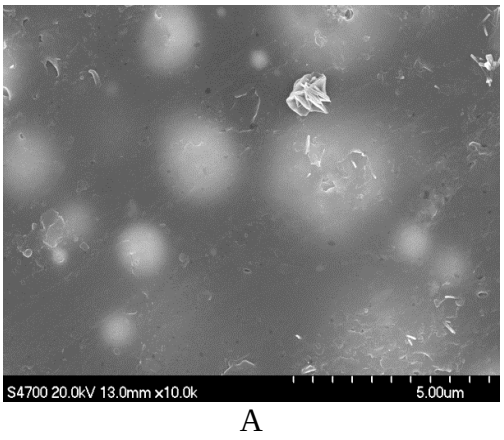

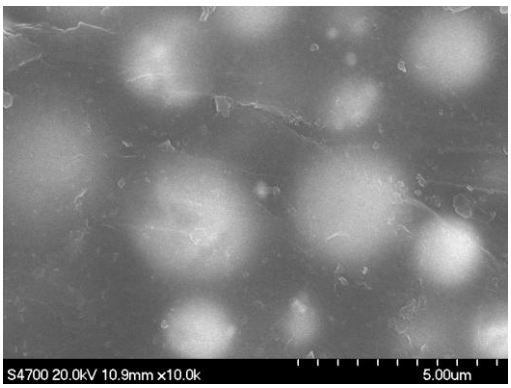

B

Figure 2. Back morphology of the zinc-rich paint after 47 days of immersion in 3.5% NaCl solution, (a) Under cathodic polarization, (b) At open circuit potential

Hence the cross-linked structure in sample B would be damaged by CP. Fig. 2 shows the back morphology of the ZRP with and without CP. No obvious hole appears in the two samples. This may be explained by the good electrical conductivity between the zinc particles in ZRP and the substrate [12], which leads part of the oxygen reduction taking place on the zinc particles [13]. Hence the alkalinity on the steel substrate is decreased, meanwhile the pores or defects may be blocked by the corrosion products of zinc particles [14]. Hence the cross-linked structure in the ZRP is not significantly influenced by cathodic protection.

3.2 .XPS analysis of the epoxy coating samples

After immersion for 30 days in 3.5 wt.% NaCl solution, the coating was peeled off from the sample surface and the substrate surface was analyzed with XPS. As shown in Fig. 3a, two oxidation states were identified for iron: Fe^0 (the metallic substrate) and Fe^{2+} (Fe_2O_3). The Fe 2p3/2 peak at 707.0 eV corresponds to iron in metallic state and the binding energy of Fe^{2+} 2p3/2 is around 710.0 eV [15]. Fig. 3b shows only one oxidation state (Fe_2O_3), indicating that the oxide film on sample B is thicker.

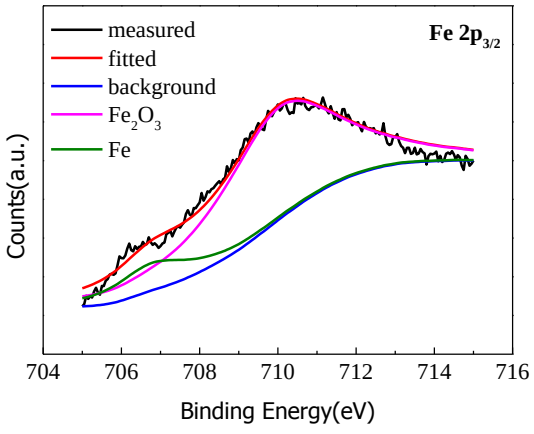

A

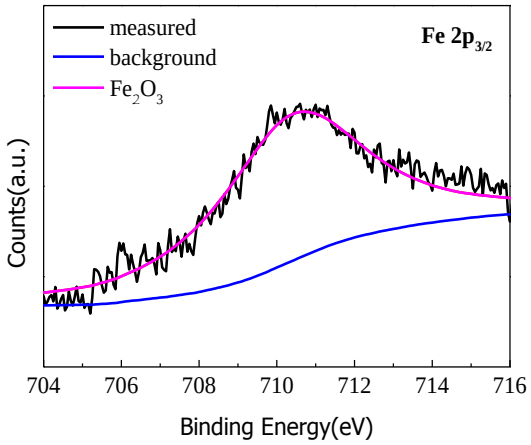

B

Figure 3. Fitted Fe2p3/2 XPS spectra of the steel surface after 30 days of immersion in 3.5% NaCl solution, (a) Sample A, (b) Sample B

This may be attributed to the strongly alkaline environment on the coating/substrate interface of sample B.

3.3. EIS measurements

Fig. 4 shows the EIS results of the four samples in 3.5 wt% NaCl solution. In the beginning for the sample coated with epoxy coating (sample A) the Nyquist plot shows only one capacitive semi-circle. However, after 6 h of immersion two semi-circles may be observed clearly (Fig. 4a), indicating that water and oxygen have reached the substrate surface and the electrochemical reactions at the metal/coating interface took place [16]. After 72 h of immersion, the Nyquist plot of sample A showed a tail, which may be explained by the coating barrier performance against the diffusion of corrosion products from the metal surface towards the coating. Meanwhile the diffusion process may become a control procedure in Faradaic processes [17]. The low-frequency |Z| value of specimen A decreased with time, indicating that the protective property of the coating decreased. After longer exposure time, 792 h, the low-frequency |Z| values of sample A decreased to $1\times10^6\ \Omega\ cm^2$ and rusty spots were seen on the steel surface under the coating, indicating the coating failure on sample A [18]. As shown in Fig. 4b, the variation trend of the Nyquist plots for sample B is similar to that for sample A. However, after 456 h of immersion, the low-frequency |Z| values of sample B already decreased to $1\times10^6\ \Omega\ cm^2$, suggesting the coating failure of sample B. Therefore, above results show that the service life of the epoxy coating on steel substrate under CP is shorter than that of the epoxy coating without CP

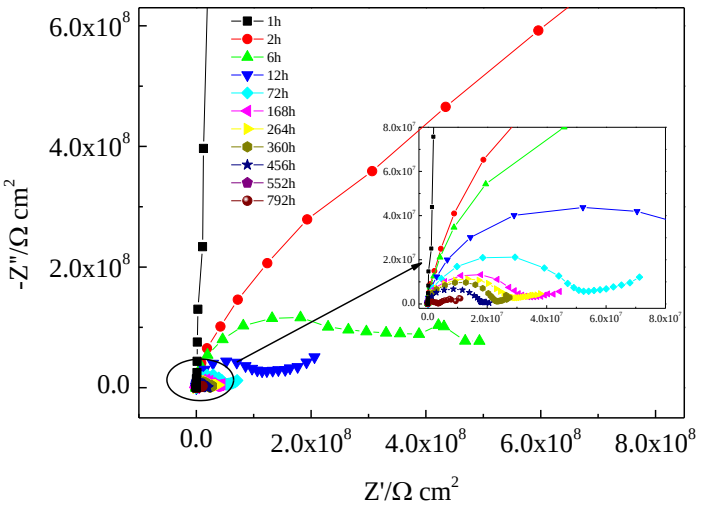
1h
2h
6h
12h
72h
168h
264h
360h
456h
552h
792h
-Z''/Ω cm2
Z'/Ω cm2
0.0
2.0x10^8
4.0x10^8
6.0x10^8
8.0x10^8

A

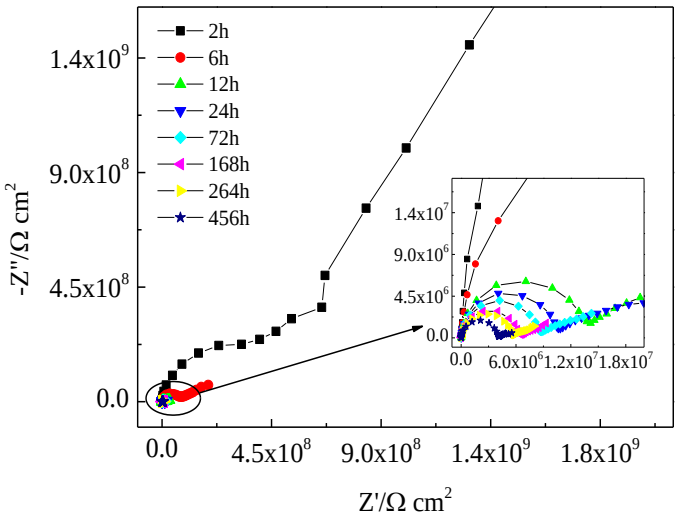
2h
6h
12h
24h
72h
168h
264h
456h
-Z''/Ω cm2
Z'/Ω cm2
0.0
4.5x10^8
9.0x10^8
1.4x10^9
1.8x10^9
6.0x10^6
1.2x10^7
1.8x10^7

B

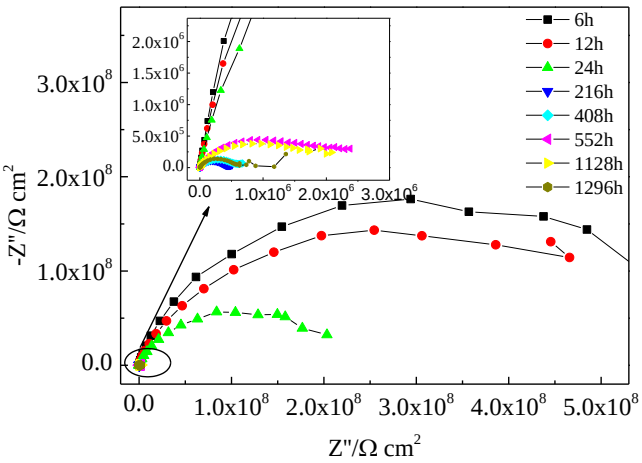
6h
12h
24h
216h
408h
552h
1128h
1296h
-Z''/Ω cm2
Z''/Ω cm2
0.0
1.0x10^8
2.0x10^8
3.0x10^8
4.0x10^8
5.0x10^8
1.0x10^6
2.0x10^6
3.0x10^6

C

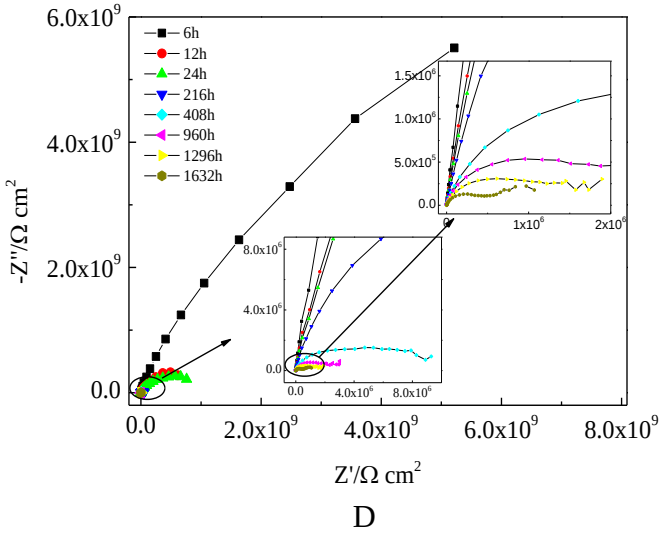

D

Figure 4. EIS spectra of the samples after different immersion times in 3.5% NaCl solution, (a) Sample A, (b) Sample B, (c) Sample C, (d) Sample D

As shown in Fig. 4c, during the initial immersion, the Nyquist plot of ZRP coated steel without CP showed one semi-circle, which is attributed to the barrier characteristic of the coating. With elapse of the immersion time, the diameter of the semi-circle decreased gradually and two capacitive semi-circles can be observed, which might be explained by the permeation of the electrolyte into the coating and the activation of zinc particles. After 408 h of immersion, the diameters of the two semi-circles increased gradually. This phenomenon may be attributed to the improved barrier property of the primer. The barrier property of the primer would be improved by deposition of the zinc corrosion products in the primer. However, the cathodic protection of the primer for the substrate would be weakened by the zinc corrosion products [8]. After 552 h of immersion, the diameters of the two semi-circles decreased again, showing the coating protective property decreased. After longer exposure time, 1296 h, the Nyquist plot of sample C showed several time constants, which could be attributed to corrosion of the steel substrate, meanwhile coating blisters on sample C were found. For sample D, during initial immersion, only one time constant was observed in Fig. 4d, which is attributed to the barrier characteristic of the coating. With the elapse of time, the diameter of the semi-circle decreased gradually. Different from sample C, the semi-circle diameter of sample D showed no increase during immersion, indicating that there was no significantly strengthened barrier stage by the deposition of the zinc corrosion products. After 1632 h of immersion, two semi-circles were observed on the Nyquist plot and the low-frequency |Z| value of sample D decreased to 1×10^6 Ω cm^2, suggesting the coating failure.

The EIS spectra can be fitted well using the equivalent circuits (EEC) shown in Fig. 5. During the first 6 h of immersion the epoxy coating (sample A) exhibited one capacitive loop, indicating the intact coating at the beginning. However, from 6 h to 168 h, two capacitive loops may be observed and the EIS spectra of sample A was fitted well using model A (Fig. 5a). The equivalent circuit consists of the coating capacitance Q_c, the coating resistance R_c, the double-layer capacitance Q_{dl}, and the charge-

transfer resistance R_{ct}. After 168 h of immersion, model A does not fit the EIS data well due to the accumulation of corrosion products at the metal/coating interface.

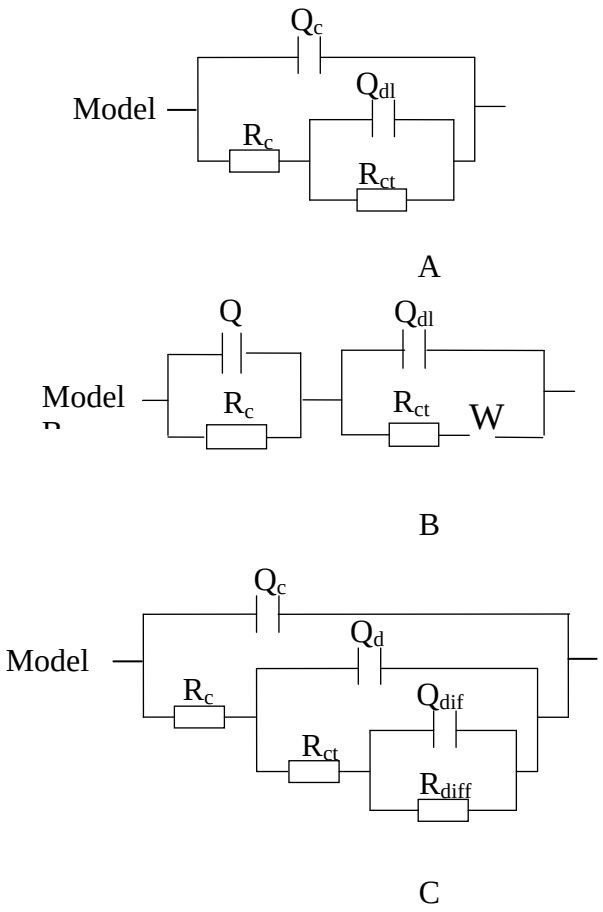

Figure 5. Equivalent electrical circuits for EIS spectra of the coatings immersed in 3.5% NaCl solution

Taking the diffusion process into account, Model B (Fig. 5b), including Warburg resistance W, provides a good fitting result [19]. During the first 6 hours, the EIS spectra of sample B can be fitted well using model A. After the beginning period of immersion, the EIS spectra could be explained using model B. Fig. 6a shows the variations of coating resistance R_c for epoxy coating with immersion time. In the initial immersion, the epoxy coating resistance R_c decreased rapidly because of penetration of the electrolyte. Then the R_c value decreased more slowly than before, which might be explained by the blockage of pores or defects by corrosion products [20]. Compared with sample A, sample B had a much low coating resistance R_c after the same immersion time. The protection property of the epoxy coating for sample B was worse than that for sample A. Since there is no pigment in the epoxy coating, the deterioration of the organic resin might be the main reason for the coating failure. At the coating/substrate interface, the cathodic protection generated strong alkalinity, which accelerated the deterioration of the epoxy coating for sample B.

For the initial immersion (6 h -24 h), the EIS spectra of sample C was fitted well using model A. After the beginning period of immersion, the EIS spectra could be explained in terms of Model C

(Fig. 5c), in which C_{diff} is the diffusion CPE and R_{diff} is the diffusion resistance. Meanwhile, Model C fits the EIS data of sample D well during the entire immersion period.

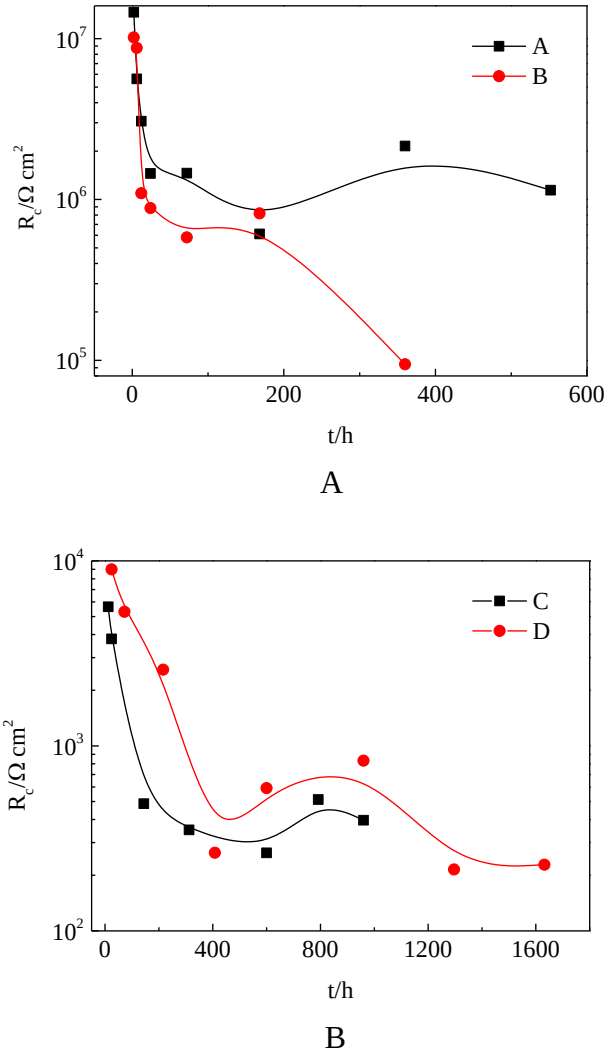

A

B

Figure 6. The variations of the coating R_c values with time, (a) The epoxy coating with or without CP, (b) The ZRP with or without CP

In Fig. 6b, the coating resistance R_c values of samples C and D are plotted with the immersion time. A decrease of R_c value was found in the initial period of immersion. This situation suggests the permeation of the electrolyte into the coating and the activation of zinc particles [21]. Then, the coating resistance R_c values decreased more slowly than before, which might be explained by the blockage of pores or defects by zinc corrosion products. The variation trend of R_c for sample D is similar to that for sample C, but the R_c value of sample D is higher than that of sample C. It indicates that the protective property of the ZRP on steel surface with CP is superior to the situation without CP. Also the lifetime of the ZRP on steel surface with CP was prolonged. Fig. 7 shows the variation of R_{ct} as a function of immersion time. As the immersion time prolonged, the R_{ct} value of sample C tended to decrease, indicating the activation of zinc particles. However, a slight increase occurred after 400 h of immersion, which may be because that the corrosion products of the zinc powders restricted the active

areas on the surface of zinc powders. On the other hand, sample D had a higher value of R_{ct} during the initial immersion and no increase of R_{ct} value occurred during the whole immersion. Therefore，for the ZRP on the steel substrate under CP, it was difficult for zinc powders to be activated in the initial immersion and there was no obvious degradation of cathodic protection for zinc powders in the late immersion period.

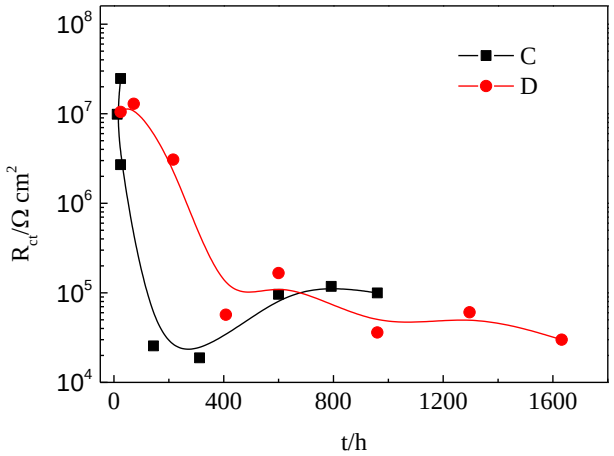

Figure 7. The variations of the obtained R_{ct} values with time for the ZRP with or without CP

3.4. Polarization current and open circuit potential

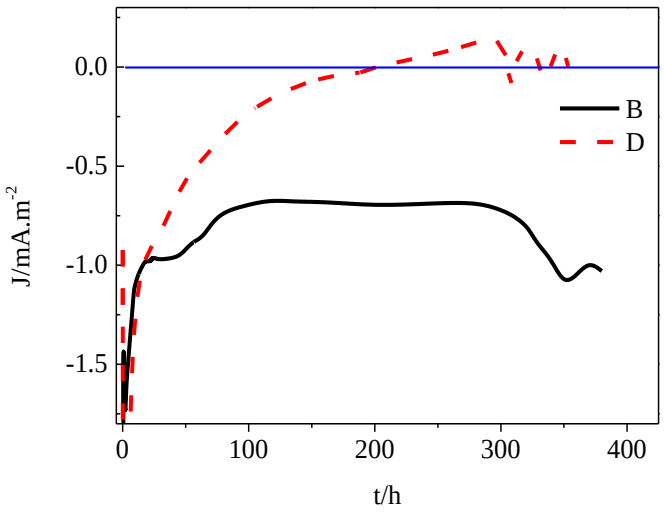

Figure 8. The variations of the polarization current density with time for the two coatings under potentiostatic polarization at -0.9 V, B-epoxy coating, D-ZRP

Fig. 8 shows the variation of the polarization current for the samples with the two different coatings under cathodic polarization at −0.9 V_{SCE} with time. During testing time, the polarization current for the epoxy coated sample under cathodic polarization at -0.9 V_{SCE} remained stable negative value. Before 300 h the polarization current density for the epoxy coated sample was about 0.7 mA/m^2.

Then the polarization current density increased rapidly to 1.1 mA/m^2, indicating decrease of the coating resistance. On the other hand, for the ZRP coated sample, Fig. 8 shows that before 200 h the polarization current was negative, suggesting that the substrate metal was under protection by the applied cathodic current. After 200 h, with the elapse of immersion time the polarization current fluctuated around the level of zero, which might be explained by that the zinc particles began to be activated and provide cathodic protection for the substrate.

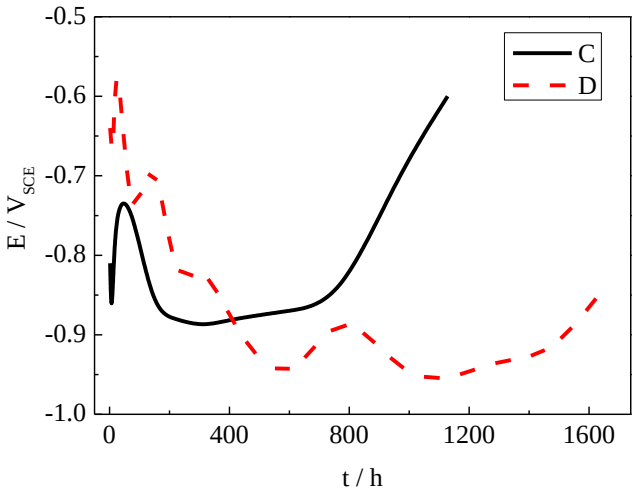

Figure 9. The variations of the E_{OCP} with time for the ZRP coated samples, C-without CP, D-with CP

Fig. 9 shows the variations of the open circuit potential of the samples as a function of immersion time. The E_{OCP} of sample D presents a trend of fluctuating downward. For sample C, after the initial period, the E_{OCP} was between -0.86 and -0.90 V_{SCE} before 700 h of immersion, which was a coupled potential between the activated zinc particles and the steel substrate. During this stage the steel substrate in sample C was cathodically protected. After about 700 h of immersion, the ZRP on sample C lost the cathodic protection property gradually. While for sample D, after the initial period the E_{OCP} was more negative, fluctuated between -0.90 and -0.95 V_{SCE} until 1600 h. Therefore, the cathodic polarization lead the potential of the steel/zinc particles system to move to the negative direction, which resulted in decreased dissolution rate of zinc particles and longer cathodic protection time. Above results indicate that the active time of zinc particles in sample D was extended because of the applied cathodic current, and the cathodic protection time provided by zinc particles was prolonged. As the result, the service life of the coating on sample D was longer than that on sample C. The results are consistent with previous EIS results.

The dissolution of zinc particles is a key factor for the cathodic protection of ZRPs. The zinc-rich coatings usually have good conductivity in order to cathodically protect the metal substrate. Hence during immersion, the potential of zinc powders in coating C was a coupled potential with the steel substrate, which was between -0.86 and -0.90 V_{SCE} according to Fig. 9. When cathodic polarization at -0.90 V_{SCE} was applied on the ZRP coated steel sample, the potential of the system (the substrate plus ZRP) was also polarized at -0.90 V_{SCE}. Therefore, after the application of polarization the potential of zinc particles was moved to the negative direction. In this condition, the dissolution rate of zinc

particles was decreased compared with the situation without applied cathodic polarization [22]. Hence the dissolution of Zn is slower in Coating D than in Coating C. As the result, coating blister was found earlier on sample C (1128 h) than on sample D (1632 h).

3.5. FT-IR analysis

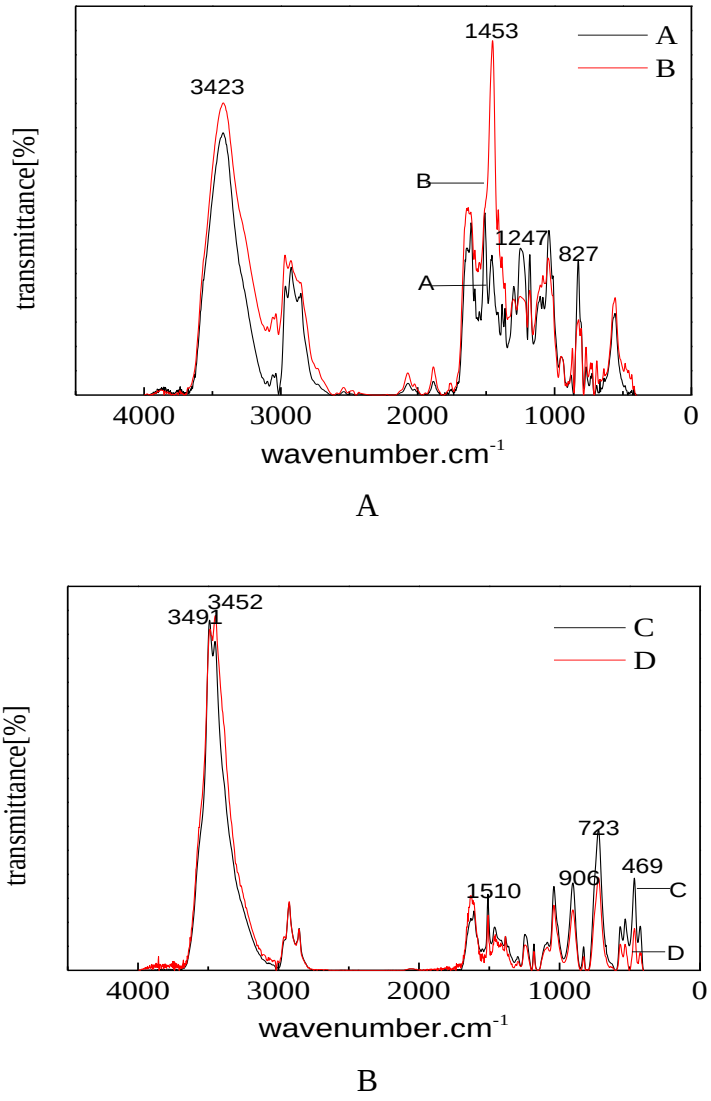

Figure 10. The FT-IR spectra of the two coatings after immersion in 3.5% NaCl solution with or without CP, (a) The epoxy coating after 30 days of immersion, (b) The ZRP after 47 days of immersion

The chemical structures of the two coatings after immersion test were analyzed with FT-IR. In order to make comparison of the individual peak of interests, all spectra were normalized using the C–H band at 2853 cm^{-1} [23]. The FT-IR spectra for the epoxy coating and the ZRP after immersion with or without CP are displayed in Fig. 10. As can be seen from Fig. 10a, comparing with sample A, the

peak intensities at 1147 cm^{-1} and 827 cm^{-1} on sample B decrease. The peak at 1147 cm^{-1} is the characteristic of C-O-C while the peak at 827 cm^{-1} can be assigned to C-H structure of epoxy group. The reduction of these peaks indicates that under cathodic protection, chain scission and epoxy hydrolyzation are accelerated. As the result the increase of the hydroxyl (–OH) and C-OH in carboxyl stretching at 3423 cm^{-1} and 1453 cm^{-1} [23,24] may be observed in Fig. 10a. On the other hand, Fig. 10b shows that after the cathodic polarization test on sample D, the hydroxyl (–OH) and C-OH peaks, which represent hydrolysis of the epoxy groups, did not show clear change, while the intensities of the peak at 469 cm^{-1} and the band at 723 cm^{-1} decrease, which are identified as ZnO and simonkolleite [$4Zn(OH)_2.ZnCl.H_2O$] respectively [25]. This result suggests that under CP the dissolution rate of zinc particles in sample D was slower, consistent with previous results. Because the very large surface area of the zinc particles in the high zinc–rich coating, during cathodic polarization the cathodic current is distributed on the surface of both the steel and the zinc particles, leading to obviously decreased cathodic current density. As the result the process of hydrolysis and depolymerization of the coating by hydroxyl would slow down. In addition, in ZRPs the formation of zinc hydroxide may also decrease the hydroxyl content to some degree.

4. CONCLUSIONS

(1) The application of cathodic polarization at −0.9 V_{SCE} on the epoxy coating increases the extent of degradation and reduces the protective properties of epoxy coating, which may be attributed to the strengthened basic environment at the coating/metal interface due to cathodic polarization.

(2) For 80 wt% zinc-rich epoxy coating, cathodic polarization at −0.9 V_{SCE} decreases the dissolution rate of the zinc particles in coating and increases the coating resistance. The activation of zinc particles is delayed and the cathodic protection time contributed by the zinc particles is prolonged. As the result the performance of the zinc-rich epoxy coating is improved by cathodic polarization.

(3) For 80 wt% zinc-rich epoxy coating, the degradation rate of the coating resin is slower than that of the epoxy coating. The presence of zinc particles in the coating would decrease the cathodic current density, reducing the local alkality, and the formation of zinc hydroxide may also decrease the hydroxyl content to some degree.

ACKNOWLEDGEMENT
The authors are grateful to the National Natural Science Foundation of China (Contact 51171014 and 51210001) for the supports to this work.

References

1. S. Amami, C. Lemaitre, A. Laksimi, S. Benmedakhene, *Corros. Sci.*, 52 (2010) 1705
2. C. Zhu, R. Xie, J.H. Xue, L.L. Song, *Electrochim. Acta*, 56 (2011) 5828
3. S. Touzain, Q.L. Thu, G. Bonne, *Prog. Org. Coat.*, 52 (2005) 311
4. D. Gervasio, I. Song, J.H. Payer, *Appl. Electrochem.*, 28 (1998) 979

5. Q.Le. Thu, H. Takenouti, S. Touzain, *Electrochim. Acta*, 51 (2006) 2491
6. E.O. Elta, J.D. Scantlebury, E.V. Koroleva, *Prog. Org. Coat*., 73 (2012) 8
7. E.O. Elta, J.D. Scantlebury, E.V. Koroleva, *Prog. Org. Coat*., 75 (2012) 79
8. A. Meroufel, S. Touzain, *Prog. Org. Coat*., 59 (2007) 197
9. H.M. Shao, W.L. Han, X.Y. Wang, Z.P. Xu, A.G. Li, *Chin. Offs. Plat*., 22 (2007) (5) 6
10. Q. Pan, L.H. Cheng, D.Z. Zhao, W. Shi, *Guangdong Chem. Industry*, 39 (2012) (13) 5
11. P.A. Sørensen, K. Dam-Johansen, C.E. Weinell, S. Kiil, *Prog. Org. Coat*., 68 (2010) 283
12. J.R. Vilche, E.C. Bucharsky, C.A. Giuudice, *Corros. Sci*., 44 (2002) 1287
13. H. Marchebois, M. Keddam, C. Savall, J. Bernard, S. Touzain, *Electrochim. Acta*, 49 (2004) 1719
14. H. Marchebois, C. Savall, J. Bernard, S. Touzain, *Electrochim. Acta*, 49 (2004) 2945
15. M.A. Hernandez, F. Gallian, D. Landolt, *Corros. Sci*., 46 (2004) 2281
16. S. González, M.A. Gil, J.O. Hernández, V. Fox, R.M. Souto, *Prog. Org. Coat*., 41 (2001) 167
17. J.T. Zhang, J.M. Hu, J.Q. Zhang, C.N. Cao, *Prog. Org. Coat*., 51 (2004) 145
18. X.Y. Lu, Y. Zuo, X.H. Zhao, Y.M. Tang, X.G. Feng, *Corros. Sci*., 53 (2011) 153
19. J.W. Hu, X.G. Li, J. Gao, Q.L. Zhao, *Mater. Desi*., 30 (2009) 1542
20. M.T. Rodríguez, J.J. Gracenea, S.J. García, J.J. Saura, J.J. Suay, *Prog. Org. Coat*., 50 (2004) 123
21. C.M. Abreu, M. Izquierw, M. Keddam, X.R. Nvoas, H. Takenout, *Elecrochim. Acta*, 41 (1996) 2410
22. D.M. Xie, J.M. Hu, S.P. Tong, J.M. Wang, J.Q. Zhang, *Acta Metallurgica Sinica*, 40 (2004) 103
23. X.F. Yang, C. Vang, D.E. Tallman, G.P. Bierwagen, S.G. Croll, S. Rohlik, *Poly. Degr. Stab*., 74 (2001) 341
24. F.X. Perrin, M. Irigoyen, E. Aragon, J.L. Vernet, *Poly. Degr. Stab*., 70 (2000) 469
25. H. Marchebois, S. Joiret, C. Savall, J. Bernard, S. Touzain, *Surf. Coat. Tech*., 157 (2002) 151